An investigation of the structure and properties of layered copper thiolates†

N. Sandhyarani and T. Pradeep*

Department of Chemistry and Regional Sophisticated Instrumentation Centre, Indian Institute of Technology, Madras 600 036, India. Fax: + +91-44-235 0509 or 2545; E-mail: pradeep@iitm.ac.in

Copper(I) n-alkane thiolate systems have been characterized using powder X-ray diffraction, IR spectroscopy, X-ray photoelectron spectroscopy and thermal analyses. The diffraction pattern is composed of a series of peaks, which are indexed to (0k0) reflections of a layered structure. The tilt angle, θ, of the alkyl chains is estimated to be 13°, distinctly different from the silver thiolates, where the chains are near normal to the silver plane. The layers interpenetrate to a small (or negligible) extent. The alkyl chain assembly is different from that of crystalline alkanes. An increase in the alkyl chain order with increase in chain length is evident in the infrared spectra. The chains are essentially all-*trans*, but *gauche* conformations are seen near the sulfur end. Upon cooling, an orientational transition occurs resulting in the freezing of the local symmetry around the methyl group. The materials show high thermal stability and desorption is seen only above 500 K. High temperature phase transitions of the materials have been studied by variable temperature powder XRD, variable temperature IR and differential scanning calorimetry. Two distinct transitions; one from an original *gauche–trans* (g–t) to a *gauche* (g) phase and another subsequent one, to a columnar mesophase, have been identified. The transitions are not fully reversible, conformational changes are observed upon heating and cooling. Thiolates appear to be model systems for the investigation of molecular self-assembly on copper surfaces.

Introduction

Redox chemistry of thiolates plays an important role in biological processes.[1] The importance of copper complexes with S donor ligands in antioxidant chemistry,[2] and as additives in lubricants[2] has accelerated the investigation of copper(I) thiolates in particular.[3,4] Organic syntheses using copper arenethiolates[5] and the semiconducting nature of a copper thiolate[6] have been reported. Thiolates can act as precursors in the solid state synthesis of chalcogenides.[7] Even though the other d^{10} complexes like silver(I) thiolates have been extensively studied,[8] literature on the structure and properties of copper thiolates is inconclusive. This is mainly because of the instability of the Cu(I) systems and the difficulties associated with the synthetic procedure. A comparison of the silver and copper thiolates has been the subject of an investigation by the group of Ellis.[9] In a recent report, it has been shown that copper thiolates possess a bilayer structure in the solid state and undergo a transition to a columnar mesophase upon increasing the temperature.[10] These layered organic–inorganic compounds are very important because of their extraordinary ability to combine organic and inorganic properties.

As a result of a number of previous studies the details of the ordering of the inorganic Ag–S substructure in silver thiolates is now well understood.[8] The pioneering study of Dance *et al.*[8a] suggested that the alkyl chains in an all-*trans* orientation are projected in either direction from a layered Ag–S lattice to make layered silver thiolates. The structure of the organic phase has been explored in detail by Parikh *et al.*[8b] The comprehensive study of Bensebaa *et al.*[8d] compared the alkyl chain assembly of thiolates with that of planar monolayers and monolayer protected clusters.

The absence of such comprehensive information on copper systems was the principal motivation to undertake this study. The similarity in the alkyl chain assembly of thiolates and monolayers also prompted this study which has been clearly brought out from the studies of silver thiolates.[8d] The silver analogues constitute a model system for the copper thiolates and it is possible to employ the methodologies used for the former for a study on the latter.

A schematic of the layered copper(I) thiolate structure is shown in Fig. 1. This structure can be considered as a result of self-assembly. Copper atoms are arranged in a plane and the sulfur atoms are attached to it from both above and below the plane. This structure can be very well correlated with the two-dimensional self-assembled monolayers (2D-SAMs) where the formation involves two processes, namely a fast adsorption and a slow self-assembly.[11] In the present case also, there are two processes; the initial strong bonding of the thiolate with copper and the three-dimensional stacking of these 2-dimensional organic–inorganic domains to an assembly leading to an organized structure as suggested for silver thiolates.[8b] The van der Waals' interactions between the alkyl chains confer stability on the system.

Experimental

Materials

CuCl$_2$·2H$_2$O, Merck, 99%, tetra n-octylammonium bromide, Merck, 98%; NaBH$_4$, octadecanethiol, octanethiol, penta-nethiol and butanethiol (all Aldrich, 99%) were used as received. AR grade solvents and deionized distilled water were used.
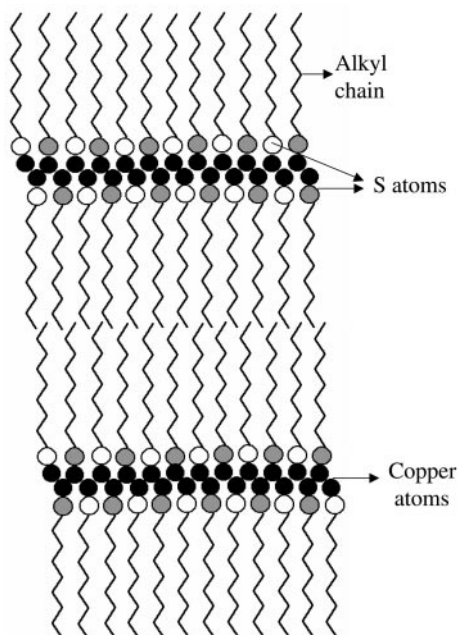
Fig. 1 Schematic of the layered structure of copper(I) thiolate. The open and shaded circles show the sulfur atoms, which are arranged alternately in two planes. Copper atoms are represented by the black spheres arranged in one plane.

Synthetic procedure

Copper alkanethiolates were prepared with octadecane, octane, pentane and butane thiols. These compounds will be referred to later as CuODT, CuOT, CuPT and CuBT, respectively. Briefly, the synthetic procedure was as follows. A 0.0358 M toluene solution (42 ml) of tetra n-octylammonium bromide was added to a vigorously stirred 0.0288 M aqueous solution (20 ml) of $CuCl_2 \cdot 2H_2O$. After 1 hour of stirring, a 0.0140 M toluene solution (45 ml) of the respective thiol was added and the resulting solution was stirred for 20 minutes. To this an aqueous solution (0.39 M, 16 ml) of sodium borohydride was added drop-wise. The solution was stirred for 15 hours and the organic layer was separated. The precipitate formed in the organic phase was collected by centrifugation. The material was washed several times with toluene and was air-dried. It was stored in the ambient laboratory air and no significant change in the spectroscopic properties was observed over the course of several weeks.

We found that the reaction was much faster compared with the literature reports.[9,10] Even though this procedure is similar to that of the metal cluster synthesis,[12] we did not see any cluster formation in these cases, as established by transmission electron microscopy and optical absorption spectroscopy. The absence of plasmon excitation at 570 nm[13] in these materials suggests that clusters have not been formed during the synthetic procedure. The quantitative mass loss in the thermogravimetric analysis confirms the formation of thiolates. Elemental analysis was used to check the purity of the products ($CuSC_4H_9$: calculated C, 31.46; H 5.94%. Found C, 31.55; H, 6.04%. $CuSC_5H_{11}$: calculated C, 36.02; H, 6.66%. Found C, 36.03; H, 6.68%. $CuSC_8H_{17}$: calculated C, 46.01; H, 8.21%. Found C, 46.02; H, 8.17%. $CuSC_{18}H_{37}$: calculated C, 61.93; H, 10.68%. Found C, 62.23; H, 10.78%).

Optical absorption spectra were collected with a Varian Cary 5E UV/VIS/NIR spectrophotometer. A suspension of copper thiolates in toluene was used for the measurements. Powder X-ray diffractograms were measured with a Shimadzu D1 200 X-ray diffractometer with Cu-Kα radiation. The samples were spread on anti-reflection glass slides to give uniform films. Variable temperature XRD measurements were performed with a Siemens diffractometer using Cu-Kα radiation. Samples

were heated to 423 K and measurements were carried out in an interval of 20°. A step size of 0.02° was used. X-Ray photoelectron spectroscopic measurements were carried out with a VG ESCALAB MkII spectrometer with Mg-Kα radiation. X-Ray flux was kept low (electron power: 70 W) in order to avoid possible beam induced damage.[14] Acquisition took about 15 minutes for each core level. All regions, C1s, S2p, and Cu2p were measured with a 50 eV pass energy. The measurements were carried out under a pressure of 10^{-8} Torr. Thick films of the samples (spread on nickel sample stubs) were used for the measurements. Infrared spectra were measured with a Bruker IFS 66v FT-IR spectrometer. Samples were prepared in the form of pressed KBr pellets. All spectra were measured with a resolution of 4 cm^{-1} and were averaged over 200 scans. Variable temperature measurements were performed with a home-built heater and a programmable temperature controller. At each temperature, the sample was allowed to equilibrate for 10 minutes before taking the measurements. The thermogravimetric (TG) data were acquired with a Netzsch STA 409. About 10 mg of the sample was used for each measurement. Measurements in the range of 323–873 K were conducted under a nitrogen atmosphere at a scan speed of 20 K min^{-1}. Differential scanning calorimetry (DSC) data were taken with a Netzsch PHOENIX DSC204 instrument. 10 mg of the sample encapsulated in an aluminium pan was used for each measurement with a scan speed of 10 K min^{-1}.

Results and discussion

In Fig. 2 we show the powder XRD patterns of the longer chain thiolates. Both the compounds show a progression of reflections, which are successive orders of diffraction from a layered structure with large d spacing. There are also weak reflections at higher 2θ due to the intralayer structure. Intense diffraction patterns with large d spacing can be interpreted in terms of three-dimensionally stacked layers of Cu and S atoms with a large interlayer lattice dimension. Each layer of Cu is separated from the other by twice the length of the alkyl chain. All these reflections are indexed as $(0k0)$ and the reflections are assigned in the figure. The interlayer spacings derived are 15.875, 17.656, 25.362 and 49.730 Å for CuBT, CuPT, CuOT and CuODT, respectively. The data fit the model in which parallel slabs of Cu and S atoms are not coplanar. The slabs contribute a small thickness, $2t_1$, to the layer as in the case of
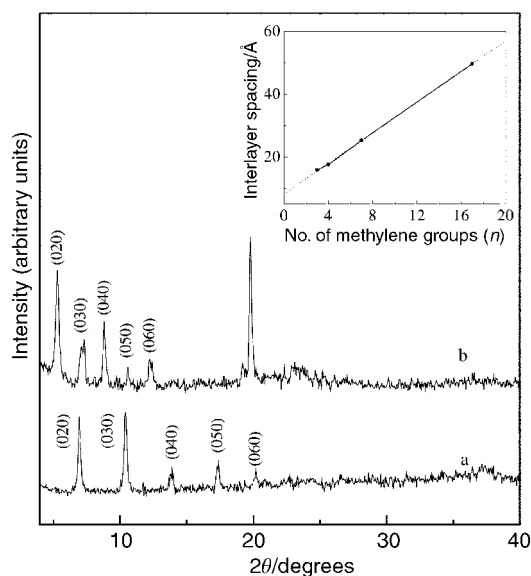

Fig. 2 The Cu-Kα powder diffraction patterns of (a) CuOT and (b) CuODT. The reflections are labeled. The inset shows the plot of interlayer spacing *versus* the number of methylene groups, *n*. A linear regression fit is used.

silver(i) thiolates.[8b] The calculated thickness of the layer (T_{cal}) is $2t_1 + 2t_2$, where $t_2 = L + r_w(CH_3) \times \cos \theta$. Here L is the length of the alkyl chain and $r_w(CH_3)$ is the van der Waals' radius of the CH_3 group (2.0 Å) and θ is the tilt angle. The observed and calculated thickness of the layer (T_{obs} and T_{cal}) for CuODT are 49.730 Å and 49.181 Å, respectively ($T_{obs} = kd$, where k is the order of diffraction). For T_{cal}, a tilt angle of 13° is assumed (see below), and t_1 has been neglected as it is relatively low in this situation. The fact that T_{obs} is greater than T_{cal} rules out the possibility of extended interdigitation, however, the terminal CH_3 groups may be interpenetrating between the layers (see below). For CuOT, T_{obs} and T_{cal} are found to be 25.362 Å and 24.194 Å and for CuPT these values are 17.656 Å and 17.250 Å, respectively. For CuBT the values are 15.875 Å and 14.200 Å. The difference between the values is larger in lower member thiolates, although there is no systematic trend. These values are slightly different from those reported by Espinet et al.[10]

In the inset of Fig. 2, a plot of interlayer spacing versus the number of methylene groups (n) in the molecule is shown. We observed a linear relationship with a slope of 2.439 Å per pair of CH_2 groups and a y-intercept of 7.960 Å. Linear correlation and the monotonic dependence of interlayer spacing with the number of methylene units indicates that all these materials possess a common structure. We compared the observed slope with an idealized model in which the alkyl chains are fully extended and are in an all-trans orientation, perpendicular to the Cu–S slab. This model gives a chain length of 1.253 Å per CH_2 group.[8b] From the slope we calculated the tilt angle, $\theta = \cos^{-1}(m_{obs}/2 \times 1.253)$, where m_{obs} is the slope of the line and 1.253 is the length of one methylene group (in Å), assuming an all-trans conformation.[8b] We estimated the tilt angle to be 13°, which is the same as that of a 2D-SAM on copper.[5] In silver thiolates, the tilt angle was calculated to be 0–5°.[8b] This difference from the silver thiolates suggests a difference in both the packing density and the angle between the surface normal and the S–C bond.

In order to understand the chemical state of the elements, we performed XPS investigations of the thiolates (spectra are provided in the ESI).† Positions and the extent of spin–orbit coupling between $Cu2p_{3/2}$ and $Cu2p_{1/2}$ correspond to the +1 oxidation state of copper. Absence of the configuration interaction satellite shows that all Cu(ii) species undergo reduction to Cu(i).[16] S2p occurs as a single peak at 162.0 eV BE corresponding to the thiolate BE normally seen for alkanethiol monolayers. C1s is present at 285 eV as in the case of 2D-SAMs.[11] The absence of oxygen suggests that there are no contaminants on the surface. In the case of copper metal, a clean surface is obtained only under ultrahigh vacuum conditions. The thiolate surface is similar to that of a SAM on gold where no impurities are observed even after prolonged exposure to vacuum.

Fig. 3 shows the infrared spectra of copper thiolates. The CH stretching region (Fig. 3A) is composed of the methylene and methyl symmetric and antisymmetric modes. For crystalline n-alkanes, the d^+ and d^- modes occur around 2845 cm^{-1} and 2916 cm^{-1}, respectively and with increasing disorder these peaks shift to higher frequencies.[17] In CuODT and CuOT, the d^+ and d^- modes appear at 2845 cm^{-1} and 2918 cm^{-1}, respectively, which correspond to solid n-alkane values.[17a] These bands undergo a blue shift in PT and BT. This indicates that when n is around 8 or above, the alkyl chains have more order. This is because of the increased van der Waals' interaction with increase in chain length as in the case of 2D-SAMs,[18] while the methyl modes, r^+ and r^-, remain at the same positions. In all the thiolates, these values are 2871 cm^{-1} and 2957 cm^{-1} respectively, which is different from that of the 2D-SAM.[18] In 2D-SAMs the values are found to be 2877 cm^{-1} and 2963 cm^{-1}, respectively. This shows that in thiolates even the chain termini are in a semi-frozen state. The rotational freedom of the chain termini can be better understood from the
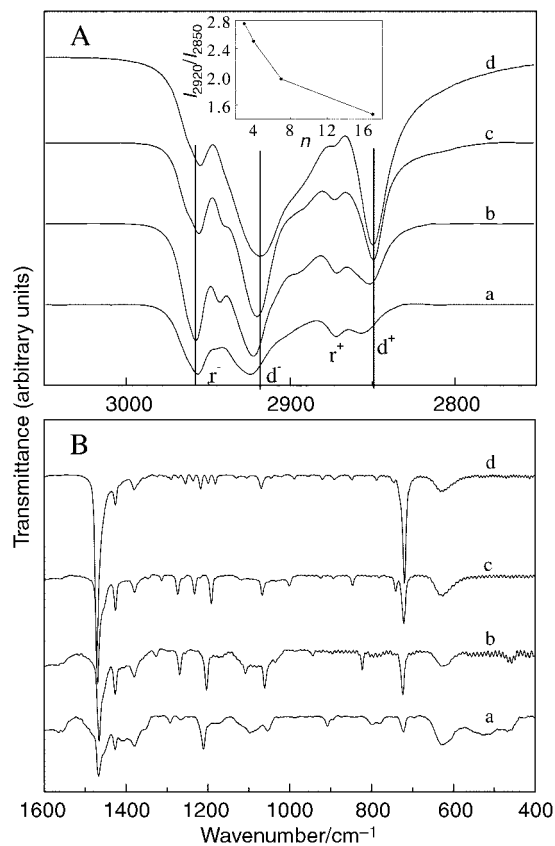
Fig. 3 High (A) and low (B) frequency FT-IR spectra of (a) CuBT, (b) CuPT, (c) CuOT and (d) CuODT. The inset of A shows a plot of the IR intensity ratio (I_{2920}/I_{2850}) versus the number of methylene units (n).

splitting of the r^- mode. It has been shown that for the two asymmetric stretching modes (r_a^- and r_b^-) to become degenerate, the CH_3 group must be in at least C_3 symmetry.[17] The splitting of the r^- modes (note the asymmetry in the peak shape for all samples) here is due to the decreased symmetry of the CH_3 group, as a result of the intermolecular interactions between the chains. As a result of this, the two asymmetric stretching frequencies are no longer degenerate. In all cases the splitting is evident, although the peaks are not distinctly resolved. Splitting is more evident in the low temperature spectra (vide infra).

The IR intensity ratio, I_{2920}/I_{2850}, can be taken as a measure of disorder,[19a] and with the increase in conformational order, this ratio decreases. The inset of Fig. 3A shows a plot of I_{2920}/I_{2850} versus the number of CH_2 groups. This shows that the ratio decreases with increasing chain length. There is a drastic decrease from C4 to C8 and the variation is slower subsequently. It can be concluded that the order increased from C4 to C8 and further increase of the chain length has only marginal effect.

Fig. 3B shows the low frequency region of these thiolates. The important vibrations of methylene group are the scissoring, wagging, twisting and rocking modes in the order of decreasing frequency. The presence of the wag–twist progression series (in the range of 1175 cm^{-1} to 1300 cm^{-1}) shows the presence of an all-trans arrangement. The peaks observed for all the thiolates between 1000 cm^{-1} and 1150 cm^{-1} are assigned to the C–C–C vibrational modes and those between 720 cm^{-1} and 980 cm^{-1} are assigned to the rocking modes. The prominent peaks in the low frequency region are the scissoring and rocking modes centered at 1463 cm^{-1} and 720 cm^{-1}. The $v(C–S)_t$ mode also appears at 720 cm^{-1}. The peak at 1423 cm^{-1} is assigned as the deformation of the methylene adjacent to sulfur. As the chain length increases, the ratio I_{1463}/I_{1423} increases, which shows that the structural integrity of the

alkanethiol is preserved during the formation of the compounds. Exact characteristics of the CH_2 scissoring (1463 cm^{-1}) and CH_3 rocking (720 cm^{-1}) modes give a sensitive measure of the packing arrangement. In polyethylene and long chain alkanes, the splitting of these bands is attributed to the intermolecular interactions between the adjacent CH_2 groups of the two chains in a crystal sub-cell.[19] This splitting is referred to as factor group splitting in an orthorhombic (odd carbon atoms) or monoclinic (even carbon atoms) arrangement. In the present case, for all samples we observed a singlet for both the modes around 1460 cm^{-1} and 720 cm^{-1}, which indicates that the unit cell is composed of only one alkyl chain. In all the thiolates, there is a prominent $v(C–S)_g$ band at 650 cm^{-1}. *This shows that the alkyl chains are not in a perfect all-trans arrangement unlike in the case of silver(1) thiolates where the v(C–S)$_g$ band is absent.*[8d] This shows that copper thiolate exists as a mixture of *gauche* (g) and *trans* (t) conformers. This high population of *gauche* conformation is also observed in alkanethiol monolayers on planar copper surfaces.[15]

The freezing of orientational freedom was observed in the low temperature IR spectra. In Fig. 4, we present the data for CuODT. In the high frequency region (Fig. 4A) the methylene modes show a distinct shift to low frequency at 150 K, the shift of the d$^+$ mode is more marked. A drastic shift is not distinct in the d$^-$ mode. Intensities of the bands progressively increase as the temperature is lowered. The r^-_a and r^-_b methyl modes are distinctly shown up in the 150 K spectrum and the splitting is more prominent as the temperature is decreased. This suggests that the transition at 150 K results in an orientationally restricted phase, leading to complete removal of the degeneracy of the CH_3 group modes. The low frequency region (Fig. 4B) does not show frequency shifts. The wagging and rocking progression modes gained intensity and the peaks are distinctly
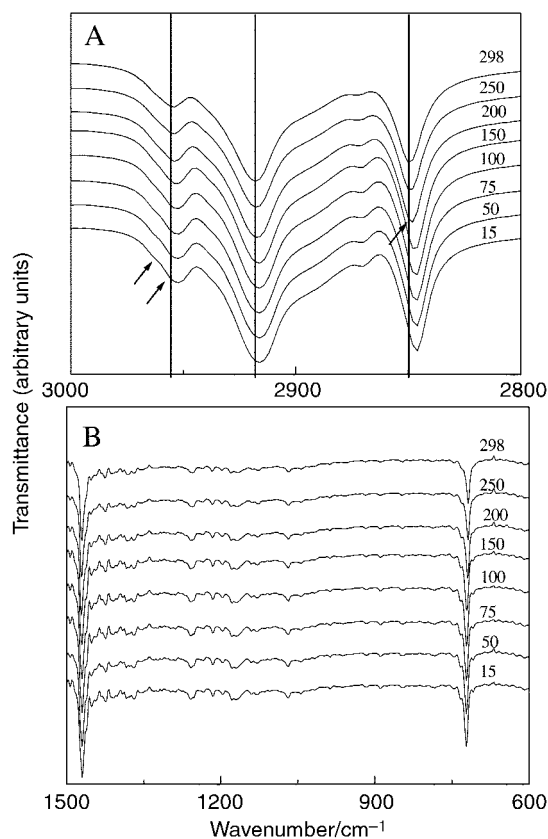
resolved indicating improved order. We do not see any splitting of the scissoring and rocking modes. This behavior is different from hydrocarbon solids[19b] and 2D-SAMs where factor group splitting of these two bands is observed at 80 K.[20] This splitting is due to the presence of two alkyl chains per unit cell. Our experiments suggest that even at 15 K, the alkyl chain assembly contains only one chain per unit cell.

The thermogravimetric data (ESI)† show mass losses of 70, 56 and 40% for CuODT, CuOT and CuPT respectively, which corresponds to a 1 : 1 ratio of copper and thiolate. In CuODT, desorption commences at around 540 K and is complete around 700 K. In the case of lower chain length thiols, desorption commences early and is complete at a lower temperature. No mass loss is seen beyond this temperature up to 900 K. The temperature dependence of the mass losses indicates that the stability of copper thiolates increases with increasing chain length. This is possibly due to the increase in the cohesive interaction between the alkyl chains with increasing chain length.

Differential scanning calorimetric traces of the thiolates (ESI)† show two distinct transitions which is consistent with the literature.[10] These transitions are attributed to the change from a crystalline (C) phase to another crystalline (C′) phase and the C′ to a columnar mesophase (M).[10] It appears that after the transition to the isotropic liquid phase, which occurs around 424 K,[10] the system is not completely reversible (not shown). Significant difference in the enthalpy is observed between heating and cooling for the C′→mesophase transition. This implies that the transition from the mesophase to the crystalline phase is incomplete. For CuOT and CuPT, only one transition is seen, which is due to the crystalline solid to the columnar mesophase transition.

In order to understand the nature of the transitions in more detail, we have performed a variable temperature powder XRD measurement. Fig. 5 shows the X-ray diffractograms of copper octadecanethiolate as a function of temperature. The splitting of the first few reflections at 7.5°, 12.3° and 20.1° suggests that the phase is an admixture of different conformations.[8c] At 343 K these doublets change to singlets. This is attributed to a solid state phase transition. The transition is observed in DSC at 323 K. Comparison with silver butanethiolate[8c] suggests that this transition could be due to the change from a g/t to a g phase. In Fig. 5 we can see the transition to the columnar mesophase[10] at 423 K, which is observed in DSC at 415 K. The emergence of two low angle peaks at this temperature shows

Fig. 4 IR spectra of CuODT at low temperatures (the temperatures used are marked in the figure). (A) CH stretching region and (B) low frequency region. The distinct shift of the d$^+$ mode and the asymmetry of the r$^-$ mode are marked.
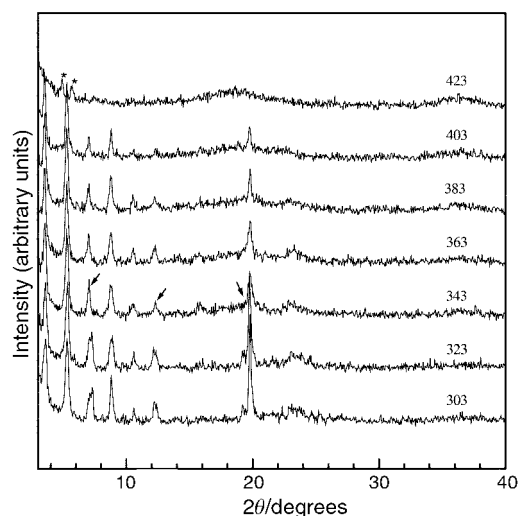

Fig. 5 Variable temperature Cu-Kα powder diffraction patterns of CuODT. Temperatures are marked in the figure. Arrows indicate the first transition resulting in the disappearance of the splitting. Asterisks in the 423 K pattern show the reflections from the columnar mesophase.

the presence of the mesophase which has been characterized before.[10] The transition observed at 423 K is consistent with the report of Espinet *et al.*[10] The columnar mesophase was characterized by the presence of four low angle rings and two diffuse halos in the diffraction pattern.[10] We see two reflections (above 2°) in the powder XRD pattern (marked with asterisks in the 423 K pattern). During cooling, the columnar mesophase changed to an amorphous phase at 403 K, and a new crystalline phase was seen below 323 K which could not be characterized completely. This behavior is different from that of silver(I) thiolates, where the transition is completely reversible.[21]

Variable temperature IR data indicate only one transition as seen in silver thiolates.[21] Many of the bands in the IR spectra of CuODT show significant changes in intensity and frequency as the temperature is varied (Fig. 6). First we shall discuss the major changes occurring in the CH stretching region. The d^+ and d^- modes present at 2845 cm^{-1} and 2918 cm^{-1} are shifted to 2856 cm^{-1} and 2926 cm^{-1}, respectively on heating from 298 K to 398 K. The shoulders disappear and merge with the intense peaks at 2856 cm^{-1} and 2926 cm^{-1} at 398 K. All these bands show an abrupt decrease in intensity as a result of the melting transition. The ratio I_{2920}/I_{2850} can be used as a measure of order–disorder transitions.[17b] The inset for Fig. 6 shows a plot of the IR intensity ratio (I_{2920}/I_{2850}) *versus* temperature. From the plot, it can be seen that the ratio increases after 373 K for CuODT. All the other thiolates studied behave similarly. This increase in ratio is due to both the reduced inter-chain vibrational coupling and the increase in twisting rotational mobility of the individual alkyl chains,
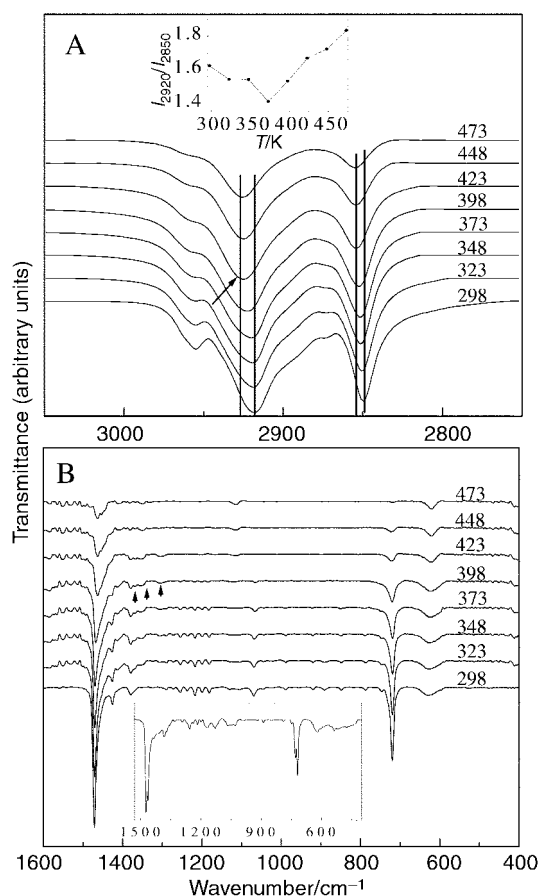
which changes the environment around a series of methylene groups.[17b] This affects the CH$_2$ scissoring mode, which in turn influences the CH stretching as they are in Fermi resonance. Band broadening indicates chain mobility, as well as the larger number of conformers present in the alkyl chains. The r^+ and r^- bands of the methyl groups are shifted to higher frequency and are also broadened along with a disappearance of the splitting in the r^- band. Thus orientational freedom exists for the chain termini at higher temperatures.[22]

In the low frequency region, the progression bands lose intensity at higher temperatures and the peak positions shift. The scissoring band became broadened and reduced in intensity as the temperature increased. The 1423 cm^{-1} peak merged with the band at 1473 cm^{-1}. All progression bands disappeared at 398 K and the CH$_3$ rocking mode (at 720 cm^{-1}) became broad with a substantial decrease in intensity (but no shift in position). In addition to all these observations, the presence of three peaks at 1367 cm^{-1}, 1353 cm^{-1} and 1343 cm^{-1} shows the conformational disorder in the system. All these bands in the progression indicate the presence of *gauche* related conformers.[17] The bands at 1367 cm^{-1} arise out of the CH$_2$ wagging vibrations in the *gauche–trans–gauche* (gtg) conformations.[17] The 1343 cm^{-1} peak is attributed to the end *gauche* conformer and that at 1353 cm^{-1} is due to the CH$_2$ wagging of the double *gauche* (gg) rotamer. All these features show that alkyl chain melting occurred at around 398 K. The ν(C–S)$_g$ band became sharper at 423 K, which shows the presence of the same conformation for all the alkyl chains. This is attributed to the presence of the mesophase at this temperature. While cooling from 423 K (*in situ*) all the features reappeared which indicates that alkyl chain melting is reversible (not shown), consistent with DSC studies. We did not see any splitting of the bands, however, upon heating the sample to 423 K and cooling to room temperature (*ex situ*), we saw the factor group splitting for both bands. The inset of Fig. 6B shows the low frequency region of CuODT after a heating/cooling cycle. This splitting of the 1473 cm^{-1} and 720 cm^{-1} bands is due to the annealing of the alkyl chains resulting in increased inter-chain interaction. It may be argued that this increase in the packing order prevents the formation of the layered thiolate structure upon cooling. This could be the reason for the non-reversibility seen in the DSC and XRD as far as the second transition is concerned.

Comparison with SAMs on planar copper surfaces

Monolayers on planar copper (2D) surfaces are structurally more complex and highly sensitive to sample preparation.[15] In copper thiolates, the copper layer is composed of Cu(I) atoms, whereas the oxidation state of metal atoms on the planar copper surface is unknown. Monolayers formed on 2D-copper surfaces are stable for less than a week, whereas layered thiolates are stable for extended periods (no decomposition was observed in two months). Alkyl chains of monolayers assembled on copper 2D surfaces are canted by ~12° from the normal to the surface, which is close to that of thiolate (~13°). A significant amount of the *gauche* conformation is present on both the surfaces, which shows that the alkanethiols are not in a complete all-*trans* arrangement unlike the case for gold or silver surfaces.[14]

Fig. 6 Variable temperature IR of CuODT. A and B show the high and low frequency regions, temperatures (in K) are marked on the spectra. Arrows indicate a shift in peak positions at 423 K. Emergence of the three peaks (at 398 K) in the low frequency region is marked. The inset of A shows the plot of IR intensity ratio (I_{2920}/I_{2850}) *versus* temperature. The inset of B shows the IR spectrum of a CuODT sample after a heating/cooling cycle between 298 K and 423 K.

Summary and conclusions

Copper thiolates have been prepared by a relatively simple method and characterized with XRD, XPS, IR and thermal analyses. The powder XRD study suggests a layered structure for all the solids with an interlayer spacing of twice the length of the alkyl chain and with negligible interdigitation. From the powder XRD we calculated a tilting angle of ~13° for all the

thiolates. IR spectroscopy shows an increase in order with increase in chain length, and revealed the deviation from the all-*trans* conformation of the alkyl chains. XPS data indicated the presence of Cu(I) and S⁻ with complete absence of oxygen confirming the chemical integrity of the system. The phase transition of these thiolate compounds was studied by variable temperature powder XRD, variable temperature IR and DSC. Two transitions are seen in the DSC and XRD, which are attributed to a solid state transition from a g/t to a t form, and subsequently to a mesophase. Powder XRD shows an irreversible structural transition at 423 K which may be due to the increase in packing density as seen in *ex situ* IR. DSC shows that the transition to the mesophase is not completely reversible as seen by XRD. Thermal stability of the thiolates increases with chain length. Alkyl chain assembly in copper thiolates is distinctly similar to that in 2D monolayers on planar copper and hence thiolates can be used as model systems for the study of 2D-SAMs.

Acknowledgements

References

1 C. Chatgilialoglu and K. D. Asmus eds., *Sulfur-Centered Reactive Intermediates in Chemistry and Biology*, Plenum Press, New York, 1990.

2 See for example, J. P. Fackler, Jr., A. Elduque, R. Davila, D. Liu, T. Grant, C. McNeal, R. Staples and T. Carlson, *The Chemistry of the Copper and Zinc Triads*, eds. A. J. Welch and S. K. Chapman, 1993.

3 B. Krebs and G. Henkel, *Angew. Chem.*, 1991, **30**, 769; D. M. Knotter, D. M. Grove, W. J. J. Smeets, A. L. Spek and G. van Koten, *J. Am. Chem. Soc.*, 1992, **114**, 3400.

4 See for a review, M. D. Janssen, D. M. Grove and G. van Koten, *Prog. Inorg. Chem.*, 1997, **46**, 97.

5 M. van Klavereen, F. Lambert, D. J. M. F. Eijkelkamp, D. M. Grove and G. van Koten, *Tetrahedron Lett.*, 1994, **35**, 6135; A. Haubrich, M. van Klavereen and G. van Koten, *J. Org. Chem.*, 1993, **58**, 5849; M. van Klavereen, E. S. M. Persson, D. M. Grove, J.-E. Backvall and G. van Koten, *Tetrahedron Lett.*, 1994, **35**, 5931; M. van Klavereen, E. S. M. Persson, A. del Villar, D. M. Grove, J.-E Backvall and G. van Koten, *Tetrahedron Lett.*, 1995, **36**, 3059; M. van Klavereen, E. S. M. Persson, D. M. Grove, J.-E Backvall and G. van Koten, *Chem. Eur. J.*, 1995, **1**, 351.

6 G. N. Schrauzer and H. Prakash, *Inorg. Chem.*, 1975, **14**, 1200.

7 D. V. Khasnis, M. Buretea, T. J. Emge and J. G. Brennan, *J. Chem. Soc., Dalton Trans.*, 1995, 45.

8 I. G. Dance, K. J. Fisher, R. M. Herath Bamda and M. L. Scudder, *Inorg. Chem.*, 1991, **30**, 183; A. N. Parikh, S. D. Gillmor, J. D. Beers, K. M. Beardmore, R. W. Cutts and B. I. Swanson, *J. Phys. Chem.*, 1999, **103**, 2850; H. G. Fijolek, J. R. Grohal, J. L. Sample and M. J. Natan, *Inorg. Chem.*, 1997, **36**, 622; F. Bensebaa, T. H. Ellis, E. Kruus, R. Voicu and Y. Zhou, *Langmuir*, 1998, **14**, 6579; M. J. Beana, P. Espinet, M. C. Lequerica and A. M. Levelut, *J. Am. Chem. Soc.*, 1992, **114**, 4182.

9 F. Bensebaa, T. H. Ellis, E. Kruus, R. Voicu and Y. Zhou, *Can. J. Chem.*, 1998, **76**, 1654.

10 P. Espinet, M. V. Lequerica and J. M. M. Alvarez, *Chem. Eur. J.*, 1999, **5**, 1982.

11 A. Ulman, *An Introduction to Ultrathin Organic Films: from Langmuir Blodgett to Self Assembly*, Academic Press, New York, 1991; A. Ulman, *Chem. Rev.*, 1996, **96**, 1533.

12 M. Brust, M. Walker, D. Bethell, D. J. Schiffrin and R. Whyman, *J. Chem. Soc., Chem. Commun.*, 1994, 801; See for a recent review, M. J. Hostetler and R. W. Murray, *Acc. Chem. Res.*, 2000, **33**, 27.

13 I. Lisiecki, F. Billoudet and M. P. Pileni, *J. Phys. Chem.*, 1996, **100**, 4160.

14 C. D. Bain, E. B. Troughton, Y-T. Tao, J. Evall, M. Whitesides and R. G. Nuzzo, *J. Am. Chem. Soc.*, 1989, **111**, 321.

15 P. E. Laibinis, G. M. Whitesides, D. L. Allara, Y.-T. Tao, A. N. Parikh and R. G. Nuzzo, *J. Am. Chem. Soc.*, 1991, **113**, 7152.

16 S. Hüfner, *Photoelectron Spectroscopy*, Springer-Verlag, Heidelberg, 1995.

17 R. G. Snyder, H. L. Strauss and C. A. Elliger, *J. Phys. Chem.*, 1982, **86**, 5145; R. G. Snyder, M. Maroncelli, H. L. Strauss and V. M. Hallmark, *J. Phys. Chem.*, 1986, **90**, 5623; M. Maroncelli, S. P. Qi, H. L. Strauss and R. G. Snyder, *J. Am. Chem. Soc.*, 1982, **104**, 6237.

18 M. D. Porter, T. B. Bright, D. L. Allara and C. E. D. Chidsey, *J. Am. Chem. Soc.*, 1987, **109**, 3559; R. G. Nuzzo, F. A. Fusco and D. L. Allara, *J. Am. Chem. Soc.*, 1987, **109**, 2358.

19 N. B. Colthup, L. H. Daly and S. E. Wiberley, *Introduction to Infrared and Raman Spectroscopy*, Academic Press, New York, 1975; R. G. Snyder, *J. Mol. Spectrosc.*, 1961, **7**, 116; J. R. Nielsen and C. E. Hathaway, *J. Mol. Spectrosc.*, 1963, **10**, 366.

20 L. H. Dubois and R. G. Nuzzo, *Annu. Rev. Phys. Chem.*, 1992, **43**, 437.

21 N. Sandhyarani, M. P. Antony, G. P. Selvam and T. Pradeep, *J. Chem. Phys.*, 2000, **113**, 9794.

22 N. Camillone III, C. E. D. Chidsey, G. Y. Liu, T. M. Putvinski and G. Scoles, *J. Chem. Phys.*, 1991, **94**, 8493.